Exploring How a Generalist Pathogen and Within-Host Priority Effects Alter the Risk of Being Infected by a Specialist Pathogen

Jing Jiao* and Michael H. Cortez

Department of Biological Science, Florida State University, Tallahassee, Florida 32306

Submitted September 22, 2021; Accepted June 14, 2022; Electronically published October 7, 2022

Online enhancements: supplemental PDF.

ABSTRACT: In multihost-multipathogen communities, a focal host's risk of being infected by a particular pathogen can be influenced by the presence of other host and pathogen species. We explore how indirect interactions between pathogens at the within-host level (through coinfecting the same individual) and the between-host level (through altered susceptible host densities) affect the focal host's risk of infection. We use an SI-type epidemiological model of two host species and two environmentally transmitted pathogens where one pathogen is a specialist on the focal host and the other pathogen is a generalist. We show that monotonic, unimodal, and U-shaped relationships between the specialist and generalist infectious propagule densities (proxies of the focal host's risk of infection) are driven by the way within-host priority effects alter the production of specialist infectious propagules by infected focal host individuals. Interestingly, within-host priority effects can also lead to overcompensation in density wherein increased infected host mortality results in greater specialist infectious propagule density. We interpret these results in terms of how the focal host's risk of being infected by a specialist pathogen is affected by the presence of a generalist pathogen, its alternative host, and within-host priority effects.

Keywords: coinfection, disease risk, priority effects, within-host interactions, indirect effects.

Introduction

Across many systems, host-pathogen dynamics and levels of infection are context dependent (for reviews, see Lazzaro and Little 2009; Wolinska and King 2009) because most systems are made up of multiple host species and multiple pathogen species (Romansic et al. 2011; Hersh et al. 2012; Abdullah et al. 2017; Fiorello et al. 2017). The presence and absence of other host species in a community are likely to have context-dependent effects on levels of disease in a focal host (LoGiudice et al. 2008; Randolph and Dobson 2012; Wood et al. 2016; Rohr et al. 2019). Indeed, prior theoretical studies (Rudolf and Antonovics 2005; Keesing et al. 2006; Roberts and Heesterbeek 2018; Cortez and Duffy 2021; Cortez 2021) predict that relationships between host diversity and disease depend on the strength of interspecific host interactions, the competence of each host species, and the pathogen transmission mode. The presence or absence of other pathogen species can also affect infection levels in a focal host. For example, *Daphnia* species compete for resources in freshwater lakes and can be infected by many pathogen species (Ben-Ami et al. 2008; Bordes and Morand 2011; Auld et al. 2012). Previous studies have shown that the proportion of infected individuals in the host species *Daphnia dentifera* depends on which host and pathogen species are present in the community (Auld et al. 2014; Clay et al. 2019*b*). Other examples of context-dependent outcomes in multiple-host or multiple-pathogen systems include fish infected by multiple strains of bacterial pathogens (Pulkkinen et al. 2010), mice infected by helminths and malarial parasites (Booth 2006), nematode and bacterial infections in African buffalo (Ezenwa et al. 2010), and infections in wild bees species (Meeus et al. 2018).

The context-dependent dynamics of multihost-multipathogen communities are shaped, in part, by the indirect interactions between the pathogen species, and these indirect effects occur at multiple levels. At the between-host level, pathogens can indirectly interact through their depletion of the pool of shared susceptible individuals (Cortez and Duffy 2020). For example, if an individual host dies because of infection by one pathogen species, then that individual host cannot be infected by a second pathogen species. Pathogens can also indirectly interact by way of the interspecific interactions between the host species. For example, reduced density of one host species may reduce resource competition with a second host species, leading to increased density of the second host species, which in

* Corresponding author; email: jjiao@fsu.edu.

ORCIDs: Jiao, https://doi.org/0000-0003-2666-6452; Cortez, https://doi.org/0000-0003-2555-7684.

  https://doi.org/10.1086/721762

turn can affect infection levels of a second pathogen. Recent theory predicts that positive indirect interactions are more likely when pathogens are more specialized on different host species and when interspecific host competition is strong and asymmetric (Cortez and Duffy 2020).

Coinfecting pathogens also interact at the within-host level (Petney and Andrews 1998; Balmer and Tanner 2011; Clay et al. 2019*b*). For many coinfecting pathogens, host mortality rates, probabilities of infection, and pathogen transmission rates depend on the order of infection; these are called within-host priority effects (Goodman and Ross 1974; Lohr et al. 2010; Hoverman et al. 2013; Sandoval-Aguilar et al. 2015; Karvonen et al. 2019; Halliday et al. 2020). In particular for the *Daphnia* system, when *D. dentifera* is coinfected by the fungus *Metschnikowia bicuspidata* and the bacterium *Pasteuria ramosa*, infected individuals produce more fungal spores when infected by the bacterium first and the fungus second and produce fewer fungal spores when infection occurs in the opposite order (Clay et al. 2019*b*). Within-host priority effects can be driven by multiple mechanisms, including competition for within-host resources and the host's immune response (Halliday et al. 2018; Greischar et al. 2020). For instance, a pathogen may have higher transmission rates if being the first to infect an individual host gives the pathogen greater access to within-host resources or allows it to better evade the host's immunological response (called niche preemption; see Mordecai et al. 2016; Mabbott 2018). On the other hand, a pathogen may have a higher probability of infection if the individual host's immunological response has been suppressed by an earlier-arriving pathogen (Ezenwa 2021). For example, suppression of the immune system by nematodes facilitates tuberculosis in African buffalo (Ezenwa et al. 2010).

Previous theoretical studies have shown that indirect pathogen interactions at the between-host level (Cortez and Duffy 2020) and the within-host level (Graham 2008; Clay et al. 2019*a*, 2019*b*, 2020) can individually affect population-level disease dynamics. However, we have a limited understanding of how those indirect interactions may jointly influence disease dynamics in systems with multiple host species and multiple pathogen species. This is because prior theoretical studies either assume there is only one host species (Gao et al. 2016; Clay et al. 2019*a*, 2019*b*) or assume there are multiple host species but coinfection is not possible (Chilvers and Brittain 1972; Holt and Dobson 2006; Cortez and Duffy 2020). However, in natural systems most communities are made up of many pathogen species with overlapping host ranges where both single infections and coinfection are possible (Seabloom et al. 2015; Nørgaard et al. 2019). For instance, some *Daphnia* species can be infected by particular bacterial pathogens, whereas others can be coinfected by both bacterial and fungal pathogens (Duffy et al. 2010). Thus, there is a need for new theory that addresses how indirect interactions between pathogens at the between-host and within-host level shape population-level disease dynamics (Ezenwa and Jolles 2011; Seabloom et al. 2015).

In this study, we analyze an SI-type model with two host species and two environmentally transmitted pathogens (i.e., pathogens transmitted through infectious propagules that are released into the environment). Motivated by a particular set of *Daphnia* species and their parasites, we focus on the case where one pathogen specializes on a focal host and the second pathogen is a generalist that can infect the focal host and an alternative host. We use the model to explore how within-host priority effects influence the indirect effects of the generalist pathogen on the specialist pathogen and the focal host's risk of infection by the specialist pathogen (defined as the density of specialist infectious propagules). We interpret our results in terms of how within-host priority effects, generalist pathogens, and alternative hosts for generalist pathogens affect a focal host's risk of infection by a specialist pathogen.

Model

Our model is motivated by the multihost-multipathogen *Daphnia* system (Ebert 2005; Duffy et al. 2010; Clay et al. 2019*b*), where infected individuals shed spores into the water column and spores are consumed by susceptible and infected individuals while filter feeding. As a specific example, the focal host species *D. dentifera* can be infected by the bacterial pathogen *Pasteuria ramosa* and the fungal pathogen *Metschnikowia bicuspidata*, whereas strain specificity of the bacterial pathogen can result in other host species (e.g., *D. lumhotzi* or *Ceriodaphnia dubia*) only being infected by the fungal pathogen (Duffy et al. 2010). Thus, in this context the bacterium is a specialist pathogen of the focal host species, and the fungus is a generalist pathogen of the focal and alternative host species. Other examples of environmentally transmitted pathogens include whirling disease in fish (Hedrick et al. 1998; Bartholomew and Reno 2002) and trematode parasites of snails (Johnson et al. 2012).

We model the epidemiological dynamics of two hosts species and two environmentally transmitted pathogens using an SI-type model; see the model diagram in figure 1. We refer to the host species as the "focal" host and the "alternative" host; they have subscripts F and A, respectively. We assume that pathogen 1 is a specialist that can infect only the focal host and that pathogen 2 is a generalist that can infect both host species (here, the pathogen's number denotes how many host species it can infect). The model describes the changes in the total density of each host species (N_F, N_A), the densities of individuals singly infected

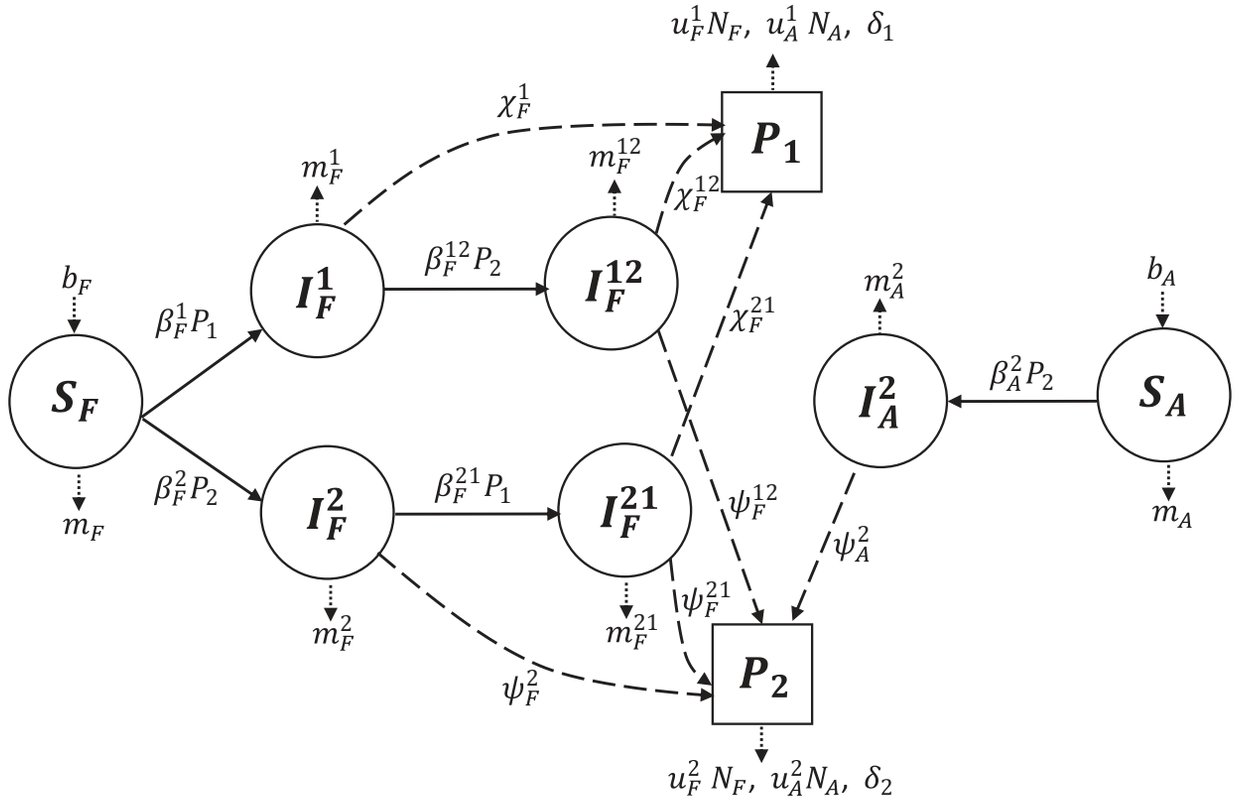

Figure 1: Diagram for model (1), where pathogen 1 specializes on the focal host and the generalist pathogen 2 can infect the focal and alternative hosts. Subscripts F and A denote the focal and alternative host species, respectively; subscripts and superscripts 1 and 2 denote the specialist and generalist pathogens, respectively. Circles denote susceptible (S_F, S_A), singly infected (I_F^1, I_F^2, I_A^2), and coinfected (I_F^{12}, I_F^{21}) individuals. Squares denote specialist (P_1) and generalist (P_2) infectious propagules. Solid lines denote changes in infection status, dashed lines denote shedding of infectious propagules, and dotted lines denote birth and mortality of hosts and degradation and uptake of infectious propagules. See table 1 for parameter definitions.

with the specialist (I_F^1) and generalist (I_F^2, I_A^2), and the densities of focal host individuals that were coinfected with pathogen j first and pathogen k second (I_F^{jk}); the densities of susceptible individuals in the focal and alternative host populations are $S_F = N_F - I_F^1 - I_F^2 - I_F^{12} - I_F^{21}$ and $S_A = N_A - I_A^2$, respectively. The model also describes the changes in specialist (P_1) and generalist (P_2) infectious propagule densities. Infection occurs when susceptible individuals encounter infectious propagules that were shed into the environment by infected individuals. The model assumes that (i) only the focal host can be (co)infected by both pathogens, (ii) both host populations have fixed total densities, and (iii) there is no recovery from infection. The first assumption allows us to focus on how within-host priority effects in a single host species scale up to affect population-level dynamics, which eliminates the potential complications of priority effects in multiple host species. The second assumption simplifies the model analysis by removing the effects of host demography and by removing the indirect effects between pathogens that are mediated by interspecific host competition. This can affect the signs of the indirect effects at the between-host level (Cortez and Duffy 2020), a point we return to in the discussion section. The third assumption simplifies the model and is motivated by the *Daphnia* system, where infections are typically lethal (Ebert et al. 2000).

The model equations are

$$\frac{dN_F}{dt} = \overbrace{b_F}^{\text{births}} - \overbrace{m_F S_F}^{\text{mortality of susceptibles}} - \overbrace{(m_F^1 I_F^1 + m_F^2 I_F^2 + m_F^{12} I_F^{12} + m_F^{21} I_F^{21})}^{\text{mortality of infecteds}}, \tag{1a}$$

$$\frac{dN_A}{dt} = \overbrace{b_A}^{\text{births}} - \overbrace{m_A S_A}^{\text{mortality of susceptibles}} - \overbrace{m_A^2 I_A^2}^{\text{mortality of infecteds}}, \tag{1b}$$

$$\frac{dI_F^1}{dt} = \overbrace{\beta_F^1 S_F P_1}^{\text{infection}} - \overbrace{\beta_F^{12} I_F^1 P_2}^{\text{coinfection}} - \overbrace{m_F^1 I_F^1}^{\text{mortality}}, \tag{1c}$$

$$\frac{dI_F^2}{dt} = \overbrace{\beta_F^2 S_F P_2}^{\text{infection}} - \overbrace{\beta_F^{21} I_F^2 P_1}^{\text{coinfection}} - \overbrace{m_F^2 I_F^2}^{\text{mortality}}, \tag{1d}$$

$$\frac{dI_A^2}{dt} = \overbrace{\beta_A^2 S_A P_2}^{\text{infection}} - \overbrace{m_A^2 I_A^2}^{\text{mortality}}, \tag{1e}$$

$$\frac{dI_F^{12}}{dt} = \overbrace{\beta_F^{12} I_F^1 P_2}^{\text{coinfection}} - \overbrace{m_F^{12} I_F^{12}}^{\text{mortality}}, \tag{1f}$$

$$\frac{dI_F^{21}}{dt} = \overbrace{\beta_F^{21} I_F^2 P_1}^{\text{coinfection}} - \overbrace{m_F^{21} I_F^{21}}^{\text{mortality}}, \tag{1g}$$

$$\frac{dP_1}{dt} = \overbrace{\chi_F^1 I_F^1 + \chi_F^{12} I_F^{12} + \chi_F^{21} I_F^{21}}^{\text{shedding}} - \overbrace{(u_F^1 N_F P_1 + u_A^1 N_A P_1)}^{\text{uptake}} - \overbrace{\delta_1 P_1}^{\text{degradation}}, \tag{1h}$$

$$\frac{dP_2}{dt} = \overbrace{\psi_F^2 I_F^2 + \psi_A^2 I_A^2 + \psi_F^{12} I_F^{12} + \psi_F^{21} I_F^{21}}^{\text{shedding}} - \overbrace{(u_F^2 N_F P_2 + u_A^2 N_A P_2)}^{\text{uptake}} - \overbrace{\delta_2 P_2}^{\text{degradation}}. \tag{1i}$$

All parameters are defined in table 1. In equations (1a) and (1b), the host populations increase because of births and decrease because of deaths of susceptible and infected individuals; the mortality rates for the infected classes account for death due to disease and sources other than disease. Because we assume fixed population sizes, the birth rate for each host species is set equal to its total mortality rate (e.g., $b_A = m_A S_A + m_A^2 I_A^2$ for eq. [1b]). In equations (1c) and (1d), the densities of singly infected focal host individuals increase when susceptible individuals become infected and decrease because of coinfection and mortality. Equation (1e) is similar except that coinfection of alternative host individuals is not possible. In equations (1f) and (1g), the densities of coinfected focal host individuals increase when singly infected individuals are coinfected and decrease because of mortality. In equations (1h) and (1i), the infectious propagule densities increase because of shedding by singly infected and coinfected individuals and decrease because of uptake and degradation.

The uptake rates account for removal of infectious propagules from the environment by all hosts. For example, in the *Daphnia* system, uptake occurs when infectious propagules are accidentally consumed by an individual host. As another example, the infectious propagules of airborne pathogens are removed from the environment when breathed in by an individual host. Because removal of an infectious propagule is necessary for it to infect an individual host, the transmission coefficient for each host class can be written as the product of the host uptake rate for the infectious propagules and the probability of infection (i.e., $\beta_i^j = u_i^j p_i^j$ for singly infected individuals and $\beta_i^{jk} = u_i^k p_i^{jk}$ for coinfected individuals, where p_i^j and p_i^{jk} are the probabilities of infection for susceptible and infected individuals). We use the more condensed notation because it is simpler. Also, for the particular *Daphnia* species and pathogens motivating our model, shedding of infectious propagules occurs only at host death. This results in the shedding rate being equal to the product of the host mortality rate and the infectious propagule burst size (e.g., $\chi_F^1 = B_F^1 m_F^1$, where B_F^1 is the number of specialist infectious propagules produced per singly infected focal host individual). We do not include this relationship in our model parameters in order to account for systems where infectious propagules are continually shed by infected individuals.

Our analysis focuses on systems at equilibrium, where equilibrium densities are denoted using asterisks (e.g., P_1^*). Throughout we assume that the equilibrium is stable, because our results are unlikely to be biologically informative when applied to an unstable equilibrium.

In model (1), the effects of coinfection and within-host priority effects are accounted for by differences in the host parameter values. Motivated by observations from empirical studies of coinfections in mice (De Roode et al. 2005), salmon (Barker et al. 2019), and *Daphnia* (Clay et al. 2019*b*), we assume that coinfection and within-host priority effects influence only the shedding rates and mortality rates of coinfected individuals. In addition, we focus only on the shedding rates of the specialist infectious propagules (χ_F^1, χ_F^{12}, χ_F^{21}) because the shedding rates for the generalist infectious propagules (ψ_F^2, ψ_F^{12}, ψ_F^{21}) do not qualitatively alter our predictions; see sections S1.4 and S2.2 of the supplemental PDF for details.

We measure the effects of coinfection and within-host priority effects in two ways. The first metric is the "total shedding rate" of each infected class. The total shedding rate for an infected class is the product of its shedding rate and its density ($\chi_F^1 I_F^1$, $\chi_F^{12} I_F^{12}$, $\chi_F^{21} I_F^{21}$). These rates define the total contribution of each infected class to the density of specialist infectious propagules. The second metric is the "lifetime shedding size" of each infected class. The lifetime shedding size of an infected class is the ratio of the shedding and mortality rate for that class

Table 1: Descriptions, units, and default values for all model variables and parameters

Quantity	Description	Unit	Value
S_i	Susceptible density for host i	Individual	Variable
I_i^j	Density of host i singly infected with pathogen j	Individual	Variable
I_i^{jk}	Density of host i coinfected with pathogen j followed by pathogen k	Individual	Variable
N_j	Total density for host i	Individual	200
P_j	Infectious propagule density for pathogen j	Propagule	Variable
b_i	Total birth rate for host i	Individual/time	Variable
m_i	Mortality rate due to nondisease sources for host i	1/time	.1
β_i^j	Transmission rate of pathogen j to susceptible individuals of host i	1/propagule/time	.01
β_i^{jk}	Transmission rate of pathogen k to host i infected with pathogen j	1/propagule/time	.01
m_i^j	Mortality rate for host class I_i^j	1/time	.5
m_i^{jk}	Mortality rate for host class I_i^{jk}	1/time	.5
χ_i^j	Shedding rate of specialist infectious propagules for host class I_i^j	Propagule/individual/time	2,000
χ_i^{jk}	Shedding rate of specialist infectious propagules for host class I_i^{jk}	Propagule/individual/time	2,000
ψ_i^j	Shedding rate of generalist infectious propagules for host class I_i^j	Propagule/individual/time	2,000
ψ_i^{jk}	Shedding rate of generalist infectious propagules for host class I_i^{jk}	Propagule/individual/time	2,000
u_i^j	Uptake rate of infectious propagule of pathogen j by host i	1/individual/time	.1
χ_i^j/m_i^j	Lifetime shedding size for singly infected individuals: total density of specialist Infectious propagules shed by a singly infected individual host before death	Propagule/individual	4,000
χ_i^{jk}/m_i^j	Lifetime shedding size for coinfected individuals: total density of specialist Infectious propagules shed by a coinfected individual host before death	Propagule/individual	4,000

Note: The host species are indexed by i (i = F for the focal host and i = A for the alternative host), and the pathogen species are indexed by j and k ($j,k = 1$ for the specialist pathogen, and $j,k = 2$ for the generalist pathogen). Values and ranges for parameters are roughly based on estimates for the *Daphnia* system (Clay et al. 2019*a*, 2019*b*).

(χ_F^1/m_F^1, χ_F^{12}/m_F^{12}, and χ_F^{21}/m_F^{21}). Each lifetime shedding size defines the average total density of infectious propagules shed by an infected individual before death. A key difference between the two metrics is that total shedding rates include exact estimates of the infected class densities, whereas the lifetime shedding sizes only indirectly estimate the densities via the mortality rates of the infected classes (i.e., the density of an infected class is approximated by the reciprocal of its mortality rate). We consider both metrics because we find that our predictions based on total shedding rates are more accurate, but we expect that it is easier to acquire estimates of lifetime shedding sizes for most empirical systems. In addition, lifetime shedding sizes align with how one would define whether the specialist pathogen has an advantage when it is the first versus second pathogen to infect a coinfected individual.

We use the shedding rates, mortality rates, and lifetime shedding sizes of the coinfected classes to define when the specialist has an advantage when coinfecting a focal individual first versus second. The specialist has a "first-arriver advantage in shedding" when coinfected individuals that were infected by the specialist first and the generalist second have a larger shedding rate of specialist propagules than coinfected individuals that were infected by the specialist second and the generalist first ($\chi_F^{12} > \chi_F^{21}$). The specialist has a "second-arriver advantage in shedding" when the inequality is reversed ($\chi_F^{12} < \chi_F^{21}$). Similarly, the specialist has a "first-arriver advantage in mortality" when coinfected individuals that were infected by the specialist first and the generalist second have smaller mortality rates than coinfected individuals that were infected by the specialist second and the generalist first ($m_F^{12} < m_F^{21}$). The specialist has a "second-arriver advantage in mortality" when the inequality is reversed ($m_F^{12} > m_F^{21}$). The specialist has a "first-arriver advantage in lifetime shedding size" when coinfected individuals that were infected by the specialist first and the generalist second have a larger lifetime shedding size than coinfected individuals that were infected in the opposite order,

$$\frac{\chi_F^{12}}{m_F^{12}} > \frac{\chi_F^{21}}{m_F^{21}}. \tag{2}$$

The specialist has a "second-arriver advantage in lifetime shedding size" when coinfected individuals that were infected by the specialist first and the generalist second have a smaller lifetime shedding size than coinfected individuals that were infected in the opposite order,

$$\frac{\chi_F^{12}}{m_F^{12}} < \frac{\chi_F^{21}}{m_F^{21}}. \tag{3}$$

Note that if the specialist has a first-arriver advantage in both shedding and mortality, then it necessarily has a

first-arriver advantage in lifetime shedding size. Similarly, if the specialist has a second-arriver advantage in both shedding and mortality, then it necessarily has a second-arriver advantage in lifetime shedding size. When the specialist has a first-arriver advantage in shedding and a second-arriver advantage in mortality or vice versa, then it can have a first- or second-arriver advantage in lifetime shedding size depending on the specific shedding and mortality rates of the coinfected classes.

We use the model to explore how the presence of the generalist pathogen affects the focal host's risk of being infected by the specialist pathogen and how that is influenced by within-host priority effects. We use infectious propagule densities as our metric for disease risk because the infection rates are proportional to the infectious propagule densities; see the $\beta_F^i S_F P_i$ and $\beta_F^{ij} I_F^i P_j$ terms in model (1). Our results focus on the relationship between the specialist (P_1) and generalist (P_2) infectious propagule densities. This allows us to assess how changes in the density of the generalist pathogen alters the density of the specialist pathogen, which in turn alters the focal host's risk of infection. In the following, we analytically compute the slope of the relationship between the specialist and generalist infectious propagule densities at equilibrium when coinfection is not possible, when coinfection is possible but priority effects are absent, and when coinfection is possible and priority effects are present. We then use numerical simulations to further explore the relationships.

Mathematical Analysis of the Model

To gain insight into how within-host priority effects alter the relationships between generalist and specialist infectious propagule densities at equilibrium, we compute the local sensitivity dP_1^*/dP_2^*. That derivative defines both the indirect effect of the generalist pathogen on the specialist pathogen and the slope of the relationship between the generalist and specialist infectious propagule densities at equilibrium. Positive values imply that the generalist has a positive indirect effect on the specialist and there is a positive relationship between generalist and specialist infectious propagule densities. In this case, increases in the generalist pathogen increase the focal host's risk of infection by the specialist pathogen. Negative values mean that the generalist has a negative indirect effect on the specialist and there is a negative relationship between generalist and specialist infectious propagule densities. In this case, increases in the generalist pathogen decrease the focal host's risk of infection by the specialist pathogen.

The methods for calculating the sensitivities were developed in Bender et al. (1984) and Yodzis (1988) and have been applied recently to epidemiological systems (Roberts and Heesterbeek 2018; Cortez and Duffy 2020, 2021; Cortez 2021). Details are provided in section S1 of the supplemental PDF. In brief, the sensitivity is computed using the ratio

$$\frac{dP_1^*}{dP_2^*} = \frac{\partial P_1^*/\partial \delta_2}{\partial P_2^*/\partial \delta_2}, \tag{4}$$

where $\partial P_1^*/\partial \delta_2$ and $\partial P_2^*/\partial \delta_2$ define how small changes in the degradation rate of generalist infectious propagules alter the equilibrium densities of specialist and generalist infectious propagules, respectively. We assume that generalist infectious propagule density decreases with increases in its degradation rate ($\partial P_2^*/\partial \delta_2 < 0$). This assumption is met in all of our numerical simulations, and we expect it to be true in most natural systems.

Systems without Coinfection

In the absence of coinfection, the indirect effect of the generalist on the specialist is

$$\frac{dP_1^*}{dP_2^*} = -C\chi_F^1 I_F^1, \tag{5}$$

where C is a positive value; see equation (S7) in section S1.2 of the supplemental PDF. Here, $\chi_F^1 I_F^1$ is the total rate of shedding by focal host individuals that are singly infected by the specialist pathogen. The sign of equation (5) shows that the indirect effect is negative. The reason is that increased density of generalist infectious propagules results in more focal host individuals becoming infected by the generalist. This decreases the density of susceptible individuals that can be infected by the specialists, which ultimately results in a decrease in specialist infectious propagule density. In total, when coinfection is not possible (or very rare), there is a negative relationship between specialist and generalist infectious propagule densities.

Systems with Coinfection and without Within-Host Priority Effects

When coinfection is possible but within-host priority effects are absent, the indirect effect of the generalist on the specialist is

$$\frac{dP_1^*}{dP_2^*} = C_c \left(\overbrace{\frac{\chi_F^c}{\beta_F^1 P_1 + m_F^c}}^{\text{term 1}} + \overbrace{\frac{-\chi_F^1}{\beta_F^1 P_1 + m_F^1}}^{\text{term 2}} \right), \tag{6}$$

where C_c is a positive value; see equation (S11) in section S1.3 of the supplemental PDF. Here, χ_F^c and m_F^c are

the shedding and mortality rates of coinfected individuals, which are independent of the order of infection. Term 1 in equation (6) is positive; it represents how increased generalist infectious propagule density leads to increased density of coinfected individuals, and hence more of the shedding of specialist infectious propagules occurs from coinfected individuals. Term 2 is negative; it represents how increased generalist infectious propagule density leads to decreases in individuals singly infected by the specialist pathogen (due to reduced densities of susceptible individuals), and hence less of the shedding of specialist infectious propagules occurs from singly infected individuals.

Equation (6) shows that the lifetime shedding sizes of singly infected individuals and coinfected individuals largely determine how the generalist pathogen affects the specialist pathogen. In particular, the indirect effect of the generalist on the specialist is negative when coinfected individuals have a smaller lifetime shedding size than singly infected individuals (term 1 is smaller in magnitude than term 2 when $\chi_F^c/m_F^c < \chi_F^1/m_F^1$). This results in a negative relationship between specialist and generalist infectious propagules, and the generalist pathogen decreases the focal host's risk of infection by the specialist. The indirect effect of the generalist on the specialist is positive when coinfected individuals have a larger lifetime shedding size than singly infected individuals (term 1 is larger in magnitude than term 2 when $\chi_F^c/m_F^c > \chi_F^1/m_F^1$). This results in a positive relationship between specialist and generalist infectious propagules, and the generalist pathogen increases the focal host's risk of infection by the specialist.

The exception to the above is that if specialist infectious propagule density is sufficiently high (P_1 large), then the shedding rates (χ_F^1, χ_F^c) approximately determine the sign of the indirect effect, not the lifetime shedding sizes (χ_F^1/m_F^1, χ_F^c/m_F^c). The reason is that the denominators of both terms in equation (6) are similar in magnitude when P_1 is large, which means the numerators of the two terms determine which term is larger in magnitude. Thus, if specialist infectious propagule density is sufficiently high, then there is a negative or positive relationship between specialist and generalist infectious propagules when singly infected individuals have higher or lower shedding rates, respectively, than coinfected individuals.

Systems with Both Coinfection and Within-Host Priority Effects

When coinfection is possible and within-host priority effects are present, the equation for the indirect effect of the generalist on the specialist (dP_1^*/dP_2^*) shows that there are 12 indirect pathways through which the generalist pathogen indirectly affects the specialist pathogen; see section S1.4 of the supplemental PDF for details. After algebraic manipulation, that equation for the indirect effect can be written as

$$\frac{dP_1^*}{dP_2^*} = \overbrace{-C_1\chi_F^1 I_F^1}^{\text{pathway 1}} + \overbrace{C_{12}\chi_F^{12} I_F^{12}}^{\text{pathway 12}} + \overbrace{C_{21}\chi_F^{21} I_F^{21}}^{\text{pathway 21}}, \tag{7}$$

where the C_i are positive values that depend on the densities of the host classes and infectious propagules; see equation (S32) in section S1.4 of the supplemental PDF for details. The three terms in equation (7) correspond to the three consolidated pathways:

$$\begin{aligned}
&\text{pathway 1: } P_2 \dashv I_F^1 \rightarrow P_1,\\
&\text{pathway 12: } P_2 \rightarrow I_F^{12} \rightarrow P,\\
&\text{pathway 21: } P_2 \rightarrow I_F^2 \rightarrow I_F^{21} \rightarrow P_1,
\end{aligned}$$

where arrows ($\rightarrow$) and turnstiles ($\dashv$) denote positive and negative direct effects, respectively. Each pathway represents the total effect of increased generalist infectious propagule density on, respectively, the densities of singly infected individuals, coinfected individuals that were infected by the specialist first and the generalist second, and coinfected individuals that were infected by the generalist first and the specialist second and how changes in the densities, in turn, affect shedding of specialist infectious propagules by each infection class. Pathway 1 is negative because increased generalist infectious propagule density decreases the density of focal host individuals that are infected by the specialist (through the reduction of susceptible host density), and hence less of the shedding of specialist infectious propagules occurs from singly infected individuals. Pathways 12 and 21 are positive because increased generalist infectious propagule density increases the densities of coinfected individuals, and hence more of the shedding of specialist infectious propagules occurs from coinfected individuals.

Equation (7) shows how the strengths of the three pathways are affected by the total shedding rate for each infected class ($\chi_F^1 I_F^1$, $\chi_F^{12} I_F^{12}$, and $\chi_F^{21} I_F^{21}$). The term for pathway 1 in equation (7) shows that the strength of pathway 1 is greater when singly infected individuals have a larger total shedding rate ($\chi_F^1 I_F^1$), which occurs with larger densities of singly infected individuals (I_F^1) or larger shedding rates by singly infected individuals (χ_F^1). This is because a larger total shedding rate for singly infected individuals means a greater reduction in specialist infectious propagule density when the density of singly infected focal host individuals decreases. The terms for pathways 12 and 21 in equation (7) show that the strengths of pathways 12 and 21 are greater when the respective coinfected classes have larger total shedding rates ($\chi_F^{12} I_F^{12}$ and $\chi_F^{21} I_F^{21}$), which occurs with larger densities of coinfected individuals (I_F^{12} and I_F^{21}) or larger shedding rates by coinfected individuals (χ_F^{12} and χ_F^{21}). This is because larger total shedding rates for coinfected individuals mean

larger increases in specialist infectious propagule density when the densities of coinfected individuals increase.

While equation (7) is conceptually straightforward, it is difficult to apply in practice because predicting the shape of the relationship between specialist and generalist infectious propagule densities requires that one can (i) accurately estimate the densities of all focal host infectious classes in an empirical system and (ii) predict how the densities of those classes change as generalist infectious propagule density increases. This is likely to be difficult to do in many empirical systems. To address this, we use the equilibrium conditions to rewrite equation (7) in terms of the lifetime shedding sizes and infectious propagule densities. This yields

$$\frac{dP_1^*}{dP_2^*} = \overbrace{-\bar{C}_1 \frac{\chi_F^1}{\beta_F^{12}P_2 + m_F^1}P_1}^{\text{pathway 1}} + \overbrace{\bar{C}_{21} \frac{\chi_F^{12}}{m_F^{12}} \frac{P_1P_2}{\beta_F^{12}P_2 + m_F^1}}^{\text{pathway 12}} + \overbrace{\bar{C}_{21} \frac{\chi_F^{21}}{m_F^{21}} \frac{P_1P_2}{\beta_F^{21}P_1 + m_F^2}}^{\text{pathway 21}}, \quad (8)$$

where the $\bar{C}_i$ are positive values that depend on the densities of the host classes and infectious propagules; see equation (S33) in section S1.4 of the supplemental PDF for details. Equation (8) shows how the strengths of the three pathways are affected by the lifetime shedding sizes of singly infected individuals (χ_F^1/m_F^1) and coinfected individuals (χ_F^{12}/m_F^{12}, χ_F^{21}/m_F^{21}) and the infectious propagules densities (P_1 and P_2). The strength of the negative effect of pathway 1 is greater when singly infected individuals have a larger lifetime shedding size (larger χ_F^1/m_F^1). In addition, the strength of the pathway 1 increases with specialist infectious propagule density (P_1 in numerator) and decreases with generalist infectious propagule density (P_2 in denominator). The strengths of the positive effects of pathways 12 and 21 are greater when coinfected individuals have larger lifetime shedding sizes (larger χ_F^{jk}/m_F^{jk}). In addition, the strengths of pathway 12 and 21 increase with increases in specialist or generalist infectious propagule density, but pathway 12 has decelerating increases with increased generalist infectious propagule density ($P_2/[\beta_F^{12}P_2 + m_F^1]$ factor), and pathway 21 has decelerating increases with increased specialist infectious propagule density ($P_1/[\beta_F^{21}P_1 + m_F^2]$ factor).

We combine the above to predict how increased generalist infectious propagule density affects (i) specialist infectious propagule density and (ii) the slope of the relationship between the specialist and generalist infectious propagule densities. Our predictions involve both the total shedding rates for each class and the lifetime shedding sizes.

First, specialist infectious propagule density is greater in the presence of the generalist pathogen only when the total shedding rate of singly infected individuals is less than the total shedding rate of all coinfected individuals (pathway 1 weaker than pathways 12 and 21 combined; $\chi_F^1 I_F^1$ smaller than $\chi_F^{12} I_F^{12} + \chi_F^{21} I_F^{21}$). At low generalist infectious propagule densities, we expect this will occur when singly infected individuals have a smaller lifetime shedding size than coinfected individuals infected by the specialist first ($\chi_F^1/m_F^1 < \chi_F^{12}/m_F^{12}$; pathway 1 weaker than pathway 12). At high generalist infectious propagule densities, we expect this to occur when singly infected individuals have a smaller lifetime shedding size than coinfected individuals infected by the specialist second ($\chi_F^1/m_F^1 < \chi_F^{21}/m_F^{21}$; pathway 1 weaker than pathway 21). In comparison, specialist infectious propagule density decreases in the presence of the generalist pathogen when the total shedding rate of singly infected individuals is greater than the total shedding rate of all coinfected individuals (pathway 1 stronger than pathways 12 and 21 combined; $\chi_F^1 I_F^1$ greater than $\chi_F^{12} I_F^{12} + \chi_F^{21} I_F^{21}$). We expect that this will occur when at least one class of coinfected individuals has a smaller lifetime shedding size than singly infected individuals ($\chi_F^{12}/m_F^{12} < \chi_F^1/m_F^1$ or $\chi_F^{21}/m_F^{21} < \chi_F^1/m_F^1$).

Second, the slope of the relationship between generalist and specialist infectious propagule density depends on pairs of the indirect pathways. When generalist infectious propagule density is sufficiently low, the negative indirect effect from pathway 1 and the positive indirect effect from pathway 12 determine the slope of the relationship. The slope of the relationship is positive when singly infected individuals have a smaller total shedding rate than coinfected individuals that were infected with the specialist pathogen first ($\chi_F^1 I_F^1 < \chi_F^{12} I_F^{12}$). We expect this will occur when singly infected individuals have a smaller lifetime shedding size than coinfected individuals that were infected with the specialist pathogen first ($\chi_F^1/m_F^1 < \chi_F^{12}/m_F^{12}$). The slope is negative when singly infected individuals have a larger total shedding rate than coinfected individuals that were infected with the specialist pathogen first ($\chi_F^1 I_F^1 > \chi_F^{12} I_F^{12}$). We expect this will occur when singly infected individuals have a larger lifetime shedding size than coinfected individuals that were infected with the specialist pathogen first ($\chi_F^1/m_F^1 > \chi_F^{12}/m_F^{12}$).

In comparison, when generalist infectious propagule density is sufficiently high, the slope of the relationship between specialist and generalist infectious propagule density is primarily determined by the magnitudes of the positive indirect effects from pathways 12 and 21. The slope of

the relationship is positive when the total shedding rate of coinfected individuals that were infected by the specialist first is smaller than the total shedding rate of coinfected individuals that were infected by the specialist second ($\chi_F^{12} I_F^{12} < \chi_F^{21} I_F^{21}$). We expect this will occur when the specialist pathogen has a second-arriver advantage in lifetime shedding size ($\chi_F^{12}/m_F^{12} < \chi_F^{21}/m_F^{21}$). The slope of the relationship is negative when the total shedding rate of coinfected individuals that were infected by the specialist first is greater than the total shedding rate of coinfected individuals that were infected by the specialist second ($\chi_F^{12} I_F^{12} > \chi_F^{21} I_F^{21}$). We expect this will occur when the specialist pathogen has a first-arriver advantage in lifetime shedding size ($\chi_F^{12}/m_F^{12} > \chi_F^{21}/m_F^{21}$).

We note two things about these predictions. First, we expect the predictions based on total shedding sizes (conditions inferred from eq. [7]) to be accurate throughout parameter space, whereas the conditions based on the lifetime shedding sizes of the infected class (conditions inferred from eq. [8]) are likely to be less accurate throughout parameter space. The reason has to do with how the two metrics estimate infected class densities, which affect the strengths of the three indirect pathways. Specifically, total shedding sizes include exact estimates of the infected class densities (e.g., I_F^1 factor in $\chi_F^1 I_F^1$), whereas lifetime shedding sizes only indirectly estimate the densities via the mortality rates of the infected classes (e.g., $1/m_F^1$ factor in χ_F^1/m_F^1). Thus, while lifetime shedding sizes are likely to be more practical to estimate than total shedding rates, the predictions based on lifetime shedding sizes may be less accurate in some cases than those based on total shedding sizes. These expectations are matched by our results from numerical simulations (see "Results from Numerical Simulations").

Second, the values C_{12} and $\bar{C}_{12}$ can be negative when specialist infectious propagule density is very low and generalist infectious propagule density is very high. This means that pathway 12 results in a negative indirect effect of the generalist pathogen on the specialist pathogen. The mechanism driving the change in sign is the following. The density of coinfected individuals that were infected by the specialist first (I_F^{12}) is very low when specialist infectious propagule density is low and generalist infectious propagule density is high. Further increases in generalist infectious propagule density increase the density of individuals singly infected by the generalist (I_F^2), which decreases susceptible focal host density. Reduced susceptible density results in reduced density of individuals that are singly infected by the specialist (I_F^1), which leads to reduced density of coinfected individuals in class I_F^{12} and reduced excretion of specialist infectious propagules by that coinfected class. We note that this change in sign does not qualitatively alter our predictions because the strength of pathway 12 is much weaker than pathway 21 in regions of parameter space where pathway 12 has a negative indirect effect.

Methods for Numerical Simulations

We used numerical simulations to explore the accuracy of our analytical predictions and illustrate different possible relationships between generalist infectious propagule density (P_2^*) and specialist infectious propagule density (P_1^*) at equilibrium. We simulated systems defined by (i) six scenarios where priority effects alter the shedding rates of specialist infectious propagules (scenarios S1–S6), (ii) six scenarios where priority effects alter the mortality rate of focal host individuals (scenarios M1–M6), and (iii) pairwise combinations of the shedding scenarios and mortality scenarios; see table 2 for details. Each shedding and mortality scenario is predicted to produce a single kind of relationship between specialist and generalist infectious propagule densities (i.e., increasing, decreasing, unimodal, or U shaped; see table 2). Scenarios S1–S3 and M1–M3 correspond to cases where the specialist pathogen has a first-arriver advantage in shedding and mortality, respectively, and scenarios S4–S6 and M4–M6 correspond to cases where the specialist pathogen has a second-arriver advantage in shedding and mortality, respectively.

For all simulations, we varied the degradation rate of the generalist infectious propagules from small ($\delta_2 = 100$) to very large ($\delta_2 = 800{,}000$) values, which causes the equilibrium density of generalist infectious propagules to vary from very large to very small values. Equilibrium densities were computed by simulating the ordinary differential equation model for 5,000 time steps, which ensured numerical convergence to equilibrium. The default parameter values for the simulations are given in table 1, and parameters with other values are specified in the figure legends. All simulations were done in R (ver. 4.1); code is available on Zenodo (Jiao and Cortez 2022).

Results from Numerical Simulations

For all of our numerical simulations, the shapes of the simulated relationships between specialist and generalist infectious propagule densities are accurately predicted by the total shedding rates of the infected classes ($\chi_F^1 I_F^1$, $\chi_F^{12} I_F^{12}$, $\chi_F^{21} I_F^{21}$). Specifically, decreasing and unimodal relationships arise when coinfected individuals that were infected by the specialist first have larger total shedding rates than coinfected individuals that were infected by the specialist second ($\chi_F^{12} I_F^{12} > \chi_F^{21} I_F^{21}$). Increasing and U-shaped relationships arise when the magnitudes of the total shedding rates are reversed ($\chi_F^{12} I_F^{12} < \chi_F^{21} I_F^{21}$). As noted earlier, a

Table 2: Scenarios of priority effects used in numerical simulations

Scenario	Rates	Type of priority effect	Pathway strengths	Predicted P_1-P_2 relationship[a]
		Shedding priority effects		
S1	$\chi_F^1 \geq \chi_F^{12} \geq \chi_F^{21}$	First-arriver advantage	$1 > 12 > 21$	Decreasing
S2	$\chi_F^{12} > \chi_F^1 \geq \chi_F^{21}$	First-arriver advantage	$12 > 1 > 21$	Unimodal
S3	$\chi_F^{12} > \chi_F^{21} > \chi_F^1$	First-arriver advantage	$12 > 21 > 1$	Unimodal
S4	$\chi_F^{21} \geq \chi_F^{12} \geq \chi_F^1$	Second-arriver advantage	$21 > 12 > 1$	Increasing
S5	$\chi_F^{21} \geq \chi_F^1 > \chi_F^{12}$	Second-arriver advantage	$21 > 1 > 12$	U shaped
S6	$\chi_F^1 > \chi_F^{21} > \chi_F^{12}$	Second-arriver advantage	$1 > 21 > 12$	U shaped
		Mortality priority effects		
M1	$m_F^1 \leq m_F^{12} \leq m_F^{21}$	First-arriver advantage	$1 > 12 > 21$	Decreasing
M2	$m_F^{12} < m_F^1 \leq m_F^{21}$	First-arriver advantage	$12 > 1 > 21$	Unimodal
M3	$m_F^{12} < m_F^{21} < m_F^1$	First-arriver advantage	$12 > 21 < 1$	Unimodal
M4	$m_F^{21} \leq m_F^{12} \leq m_F^1$	Second-arriver advantage	$21 > 12 > 1$	Increasing
M5	$m_F^{21} \leq m_F^1 < m_F^{12}$	Second-arriver advantage	$21 > 1 > 12$	U shaped
M6	$m_F^1 < m_F^{21} < m_F^{12}$	Second-arriver advantage	$1 > 21 > 12$	U shaped

[a] Predicted P_1-P_2 relationships are based on the magnitudes of the lifetime shedding sizes for the three focal host infected classes (χ_F^1/m_F^1, χ_F^{12}/m_F^{12}, χ_F^{21}/m_F^{21}).

limitation of using total shedding rates is that one needs to accurately estimate the density of each infected class (I_F^1, I_F^{12}, I_F^{21}) at each density of the specialist pathogen (P_2).

We now explore when the lifetime shedding sizes accurately and inaccurately predict the shapes of the relationships between specialist and generalist infectious propagule densities. We focus on this metric because lifetime shedding sizes are likely easier to estimate than total shedding rates in empirical systems. We start by considering the special cases where priority effects alter only either the shedding rates or the mortality rates of coinfected individuals. We then consider systems where priority effects alter both the shedding rates and the mortality rates of coinfected individuals.

We first consider systems where within-host priority effects affect only shedding rates (scenarios S1–S6) or only host mortality rates (scenarios M1–M6). Table 2 summarizes the shapes of the relationships between specialist and generalist infectious propagule densities that are predicted on the basis of the lifetime shedding sizes of each infectious class; simulation results are shown in figures 2 and 3. In nearly all simulations, the relationships between specialist and generalist infectious propagule densities qualitatively match the predictions based on the lifetime shedding sizes of each infectious class. In particular, a first-arriver advantage in shedding or mortality yields decreasing or unimodal relationships (left columns of figs. 2, 3), and a second-arriver advantage in shedding or mortality yields increasing or U-shaped relationships (right columns of figs. 2, 3). However, inaccurate predictions can arise when priority effects alter mortality rates and one coinfected class has a much higher mortality rate than the other coinfected class. Specifically, increasing relationships can arise instead of predicted U-shaped relationships if the specialist has a very large second-arriver advantage in mortality (m_F^{12} is much larger than m_F^{21}; red squares and triangles in fig. 3*D*). The predictions are inaccurate because the lifetime shedding sizes do not account for one coinfected class (I_F^{12}) being at much lower densities than the other coinfected class (I_F^{21}) for all generalist infectious propagule densities.

Now we consider systems where within-host priority effects alter both shedding rates and host mortality rates (pairwise combinations of scenarios S1–S6 and M1–M6). Simulations are shown in figures 4, 5, S1, and S2. While there are many examples where the lifetime shedding sizes of the infected classes accurately predict the qualitative shape of the relationship between specialist and generalist infectious propagule densities, there are also many examples where the lifetime shedding sizes yield inaccurate predictions. We find two different kinds of errors, with the type of error depending on how priority effects alter the shedding and mortality rates of coinfected individuals.

In the first kind of error, the lifetime shedding sizes accurately predict the sign of the slope of the relationship for large generalist infectious propagule densities but inaccurately predict the sign of the slope at small generalist infectious propagule densities. These errors typically arise in systems where the specialist has a first-arriver advantage in mortality and a first-arriver advantage in shedding (combinations of scenarios S1–S3 and M1–M3; fig. 4) or the specialist has a second-arriver advantage in mortality and a second-arriver advantage in shedding (combinations of scenarios S4–S6 and M4–M6; fig. S2). For example, unimodal relationships can arise instead of predicted decreasing relationships (curves with circles and triangles

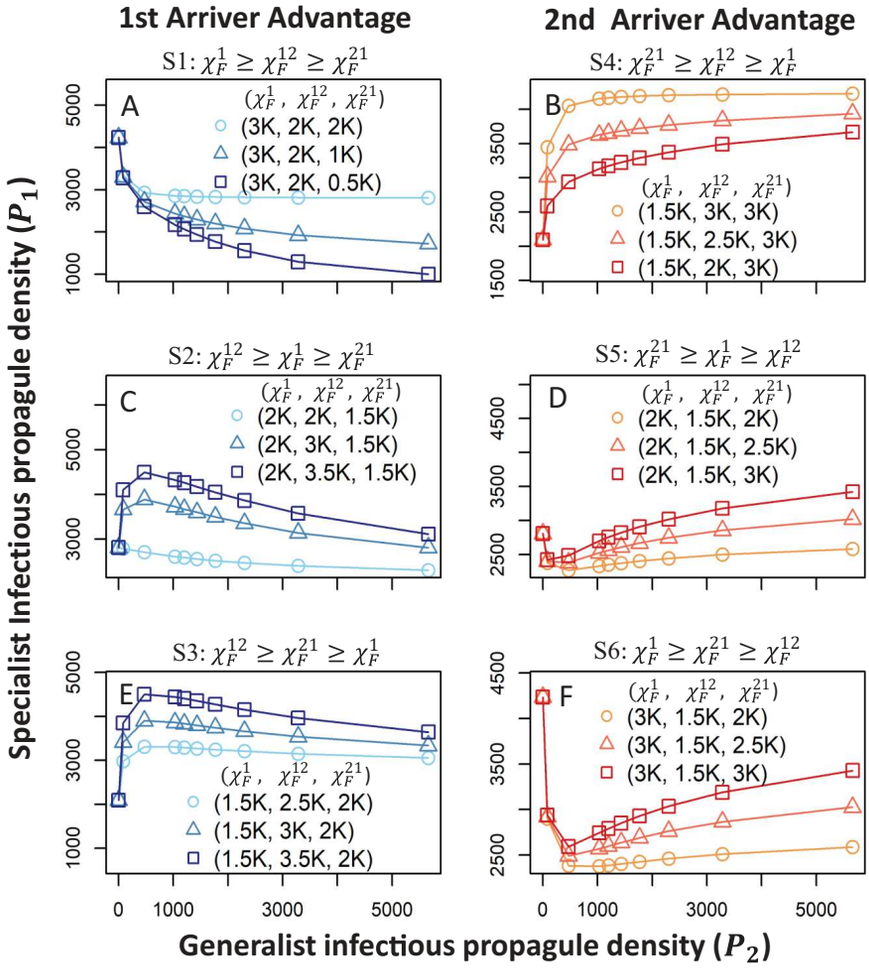

Figure 2: Relationships between generalist and specialist infectious propagule densities at equilibrium when within-host priority effects only affect the shedding rates of specialist infectious propagules. *Left column*, decreasing and unimodal relationships occur when the specialist has a first-arriver advantage in shedding ($\chi_F^{12} > \chi_F^{21}$); darker blue shades imply a greater first-arriver advantage. *Right column*, increasing and U-shaped relationships occur when the specialist has a second-arriver advantage in shedding ($\chi_F^{21} > \chi_F^{12}$); darker red shades indicate a greater second-arriver advantage. Shedding rates are indicated in the figure (where K = 1,000); all other parameters values are given in table 1.

in fig. 4*G*), and decreasing relationships can arise instead of predicted unimodal relationships (curves with circles and triangles in fig. 4*I* and all curves in fig. 4*M*). In figures 4 and S1, inaccurate predictions are made for small generalist infectious propagule densities in about 30% of the simulations; see section S2.1 of the supplemental PDF for details.

In the second kind of error, the lifetime shedding sizes accurately predict the sign of the slope of the relationship for small generalist infectious propagule densities but inaccurately predict the sign of the slope at large generalist infectious propagule densities. In our simulations, these errors always arise in systems where the specialist has a first-arriver advantage in mortality and a second-arriver advantage in shedding or vice versa (combinations of scenarios S1–S3 and M4–M6 or combinations of scenarios S4–S6 and M1–M3). For example, decreasing relationships can arise instead of predicted U-shaped relationships (curve with squares in fig. 5*G* and curves with circles in fig. 5*K*), increasing relationships can arise instead of predicted unimodal relationships (curves with triangles and squares in fig. 5*I*), and U-shaped relationships can arise instead of predicted unimodal relationships (curve with squares in fig. 5*F*). In figures 5 and S2, inaccurate predictions are made for large generalist infectious propagule densities in about 60% of the simulations; see section S2 of the supplemental PDF for details.

Altogether, these numerical results suggest that the relationships between specialist and generalist infectious propagule densities can be accurately predicted by total

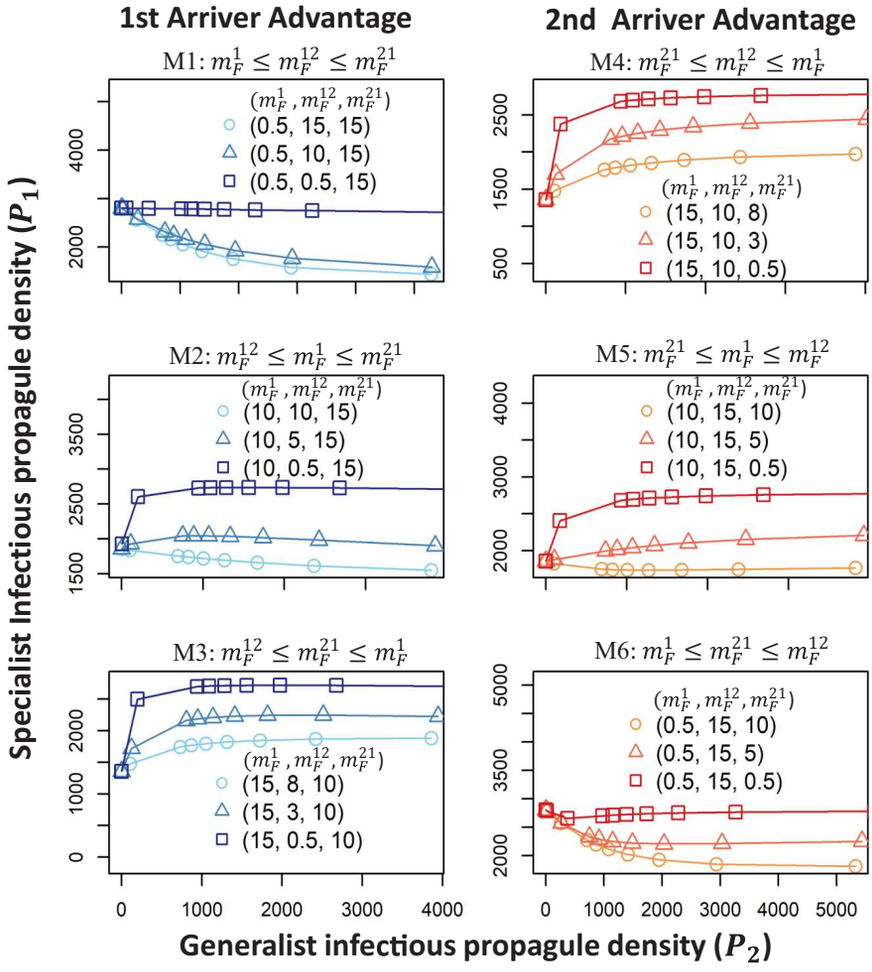

Figure 3: Relationships between generalist and specialist infectious propagule densities at equilibrium when within-host priority effects only influence mortality rates. *Left column*, decreasing and unimodal relationships occur when the specialist pathogen has a first-arriver advantage in mortality ($m_F^{12} < m_F^{21}$); darker blue shades imply a greater first-arriver advantage. Decreasing sections of the curves for $P_2 > 5{,}500$ are not shown in *E. Right column*, increasing and U-shaped relationships occur when the specialist pathogen has a second-arriver advantage in mortality ($m_F^{21} > m_F^{12}$); darker red shades indicate a greater second-arriver advantage. Mortality rates are indicated in the figure; all other parameters values are given in table 1.

shedding rates. In comparison, lifetime shedding sizes can accurately predict the qualitative shapes of the relationships in many cases, but the accuracy is much lower in systems where the specialist has different advantages in shedding and mortality (e.g., a first-arriver advantage in shedding and a second-arriver advantage in mortality). These inaccuracies arise because lifetime shedding sizes do not directly estimate the densities of the infectious classes, which results in inaccurate predictions of the strengths of the three indirect pathways.

We find one new phenomenon that can arise when within-host priority effects alter both the shedding rates and the mortality rates of coinfected individuals: increased mortality of a coinfected class can cause an increase in specialist infectious propagule density. This is an example of stage-specific overcompensation in density (de Roos et al. 2007; de Roos and Persson 2013; Jiao et al. 2016; Sorenson and Cortez 2021), wherein increased mortality of a specific stage of an organism (here, a coinfected class) leads to increased density in a different stage (infectious propagule density). In our simulations, we find that the overcompensatory response arises when the coinfected class experiencing increased mortality has a lower shedding rate than the other coinfected class. For example, specialist infectious propagule density can increase as the mortality rate m_F^{12} increases when coinfected individuals that were infected by the specialist first and generalist second have lower shedding rates than coinfected individuals that were infected

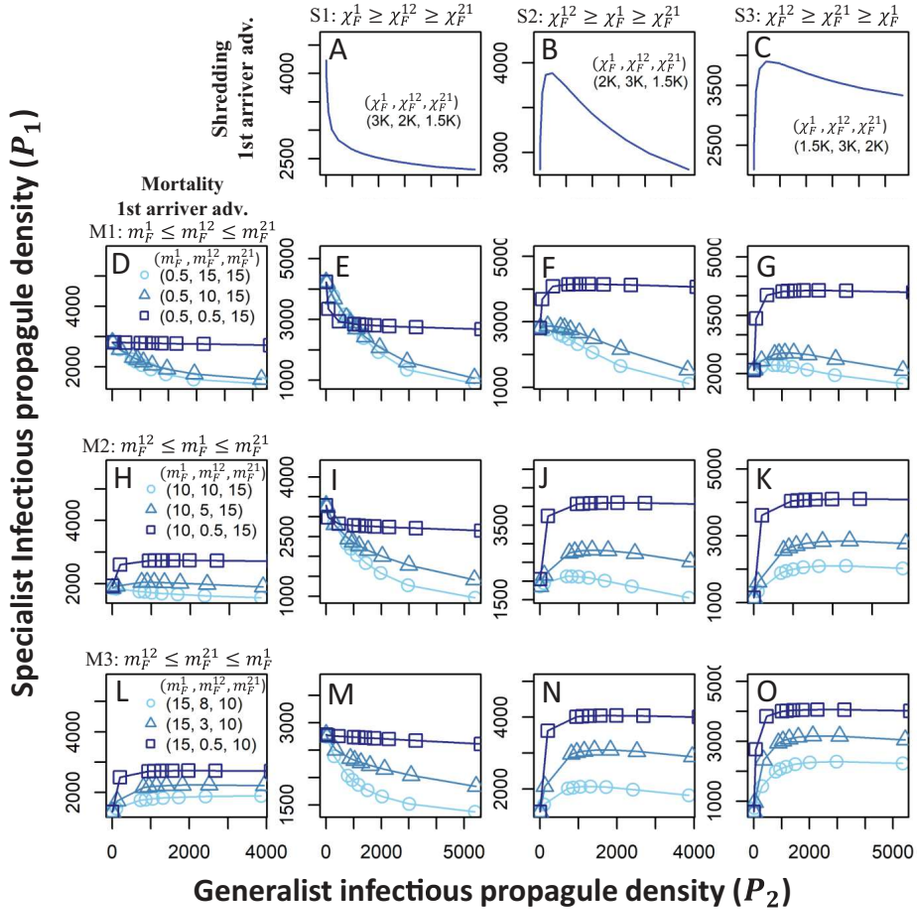

Figure 4: Relationships between generalist and specialist infectious propagule densities at equilibrium when the specialist has a first-arriver advantage in both shedding and mortality. *Top row*, relationships when priority effects only affect shedding rates. *Left column*, relationships when priority effects only affect mortality rates; darker blues indicate a greater first-arriver advantage in mortality. *E–G*, *I–K*, *M–O*, Relationships when priority effects alter both shedding and mortality rates. Curves correspond to the shedding rates in the top row and mortality rates with the same symbol and color in the left column. Darker blues indicate a greater first-arriver advantage. Table 1 defines values of unspecified parameters.

by the specialist second and generalist first ($\chi_F^{12} < \chi_F^{21}$; compare light blue and dark blue curves on the left sides of fig. 5*F*, 5*G*, 5*K* and on the right side of fig. 5*N*). Similarly, specialist infectious propagule density can increase as the mortality rate m_F^{21} increases when coinfected individuals that were infected by the specialist second have lower shedding rates than coinfected individuals that were infected by the specialist first ($\chi_F^{12} > \chi_F^{21}$; compare light red and dark red curves on the left sides of fig. S2*E*, S2*I*, S2*M*, S2*N*). The reason for the overcompensatory response is that the coinfected class with the lower shedding rate is a bottleneck stage for the pathogen. As a result, increasing the mortality rate of the bottleneck stage causes more focal host individuals to end up in the singly infected class or the other coinfected class, which leads to higher total shedding rates of infectious propagules by the focal host and higher specialist infectious propagule density.

Discussion

Disease dynamics in many multihost-multipathogen communities are context dependent (Lazzaro and Little 2009; Wolinska and King 2009), with the presence and absence of different host and pathogen species leading to different levels of disease (Booth 2006; Ezenwa et al. 2010; Pulkkinen et al. 2010; Auld et al. 2014; Clay et al. 2019*b*). We explored how the indirect interactions between pathogens at the between-host level and the within-host level jointly shape the relationships between specialist and generalist infectious propagule densities. We use infectious propagule

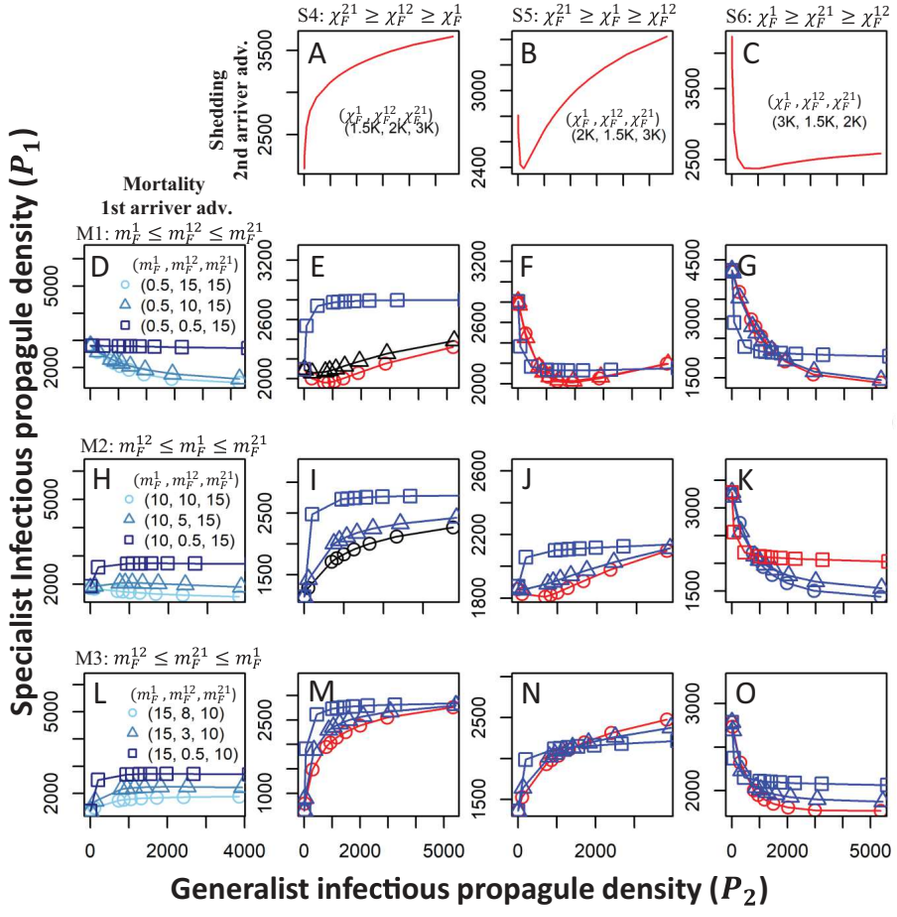

Figure 5: Relationships between generalist and specialist infectious propagule densities at equilibrium when the specialist has a second-arriver advantage in shedding and a first-arriver advantage in mortality. Panel descriptions are the same as in figure 4. In *E–G*, *I–K*, and *M–O*, curve color denotes whether the specialist pathogen has a first-arriver advantage in lifetime shredding size (blue; $\chi_F^{12}/m_F^{12} > \chi_F^{21}/m_F^{21}$), a second-arriver advantage in lifetime shredding size (red; $\chi_F^{12}/m_F^{12} < \chi_F^{21}/m_F^{21}$), or no advantage in lifetime shredding size (black; $\chi_F^{12}/m_F^{12} = \chi_F^{21}/m_F^{21}$). Table 1 defines values of unspecified parameters.

densities as proxies for the focal host's risk of infection because the infection rates in model (1) are proportional to the infectious propagule densities.

We found that the total shedding rates of singly infected and coinfected individuals ($\chi_F^1 I_F^1$, $\chi_F^{12} I_F^{12}$, $\chi_F^{21} I_F^{21}$) are key factors determining how a generalist pathogen influences a focal host's risk of infection by a specialist pathogen. This is because the total shedding rates determine the strengths of the three pathways through which the generalist pathogen indirectly affects the specialist pathogen (eq. [7]), which in turn determines the slope of the relationship between the risk of being infected by each pathogen (i.e., the relationship between generalist and specialist infectious propagule densities). Because it may be difficult to accurately measure infected class densities in empirical systems, we also explored how accurately the qualitative relationships between specialist and generalist infectious propagules could be predicted by the lifetime shedding sizes for each class (i.e., total density of specialist infectious propagules produced before death; χ_F^1/m_F^1, χ_F^{12}/m_F^{12}, χ_F^{21}/m_F^{21}). Our analytical results (eq. [8]) and numerical simulations (figs. 2–5) show that the lifetime shedding sizes can accurately predict how the generalist pathogen alters the focal host's risk of infection by the specialist in some cases, but inaccurate predictions can arise because lifetime shedding sizes do not directly estimate the densities of each infected class.

While we have focused on environmentally transmitted pathogens, our results also apply to coinfecting direct transmission pathogens (i.e., pathogens that are spread via direct contact between susceptible and infected individuals). This is because our environmental transmission model reduces to a density-dependent direct transmission model when there is no degradation of infectious

propagules ($\delta_j = 0$) and reduces to a frequency-dependent direct transmission model when there is no uptake of infectious propagules ($u_i^j = 0$; Cortez 2021; Cortez and Duffy 2021). In these cases, the focal host's risk of infection by the specialist pathogen is measured by a weighted sum of infection rates from the singly infected and coinfected classes. Thus, our results may help explain how indirect interactions between pathogens shape the context-dependent dynamics of systems with environmentally or directly transmitted pathogens.

Prior studies have explored how between-pathogen interactions can shape disease dynamics in communities with a single host species (Graham 2008; Clay et al. 2019*a*, 2019*b*, 2020). When comparing that prior work to this study, a natural question is, How does the presence or absence of an alternative host species affect the focal host's risk of infection by a particular pathogen? Our results can be translated to address that question (albeit limited to the case where the pathogen does not affect host demography); see equation (S36) and accompanying text in section S1.4 of the supplemental PDF for details. In effect, varying alternative host density from low to high values qualitatively reproduces a portion of the relationship between generalist (P_2^*) and specialist (P_1^*) infectious propagule densities; see figure 6 for an illustration. To determine what portion of the relationship between generalist (P_2^*) and specialist (P_1^*) infectious propagule densities is produced by the relationship between alternative host density (N_A) and specialist infectious propagule density (P_1^*), one must know two things: (i) the generalist infectious propagule density in the absence of the alternative host (P_2^* when $N_A = 0$) and (ii) how increases in alternative host density (P_2^*) affect generalist infectious propagule density at equilibrium (P_2^*). The first determines the left end point of the relationship between specialist infectious propagule density (P_1^*) and alternative host density N_A; compare the circle, triangle, and square in figure 6*a* with the respective shapes in figure 6*b*–6*e*. The second determines whether increased alternative host density causes generalist infectious propagule density to increase or decrease. Increased alternative host density increases generalist infectious propagule density (fig. 6*b*–6*d*) when the alternative host is a source of infectious propagules (meaning that total shedding by infected individuals is greater than the total uptake by all individuals). In contrast, increased alternative host density decreases generalist infectious propagule density (fig. 6*e*) when the alternative host is a sink for infectious propagules (meaning that total shedding by infected individuals is less than the total uptake by all individuals). Translating our results shows that increased density of an alternative host for a generalist pathogen can increase or decrease a focal host's risk of infection by a specialist pathogen, depending on

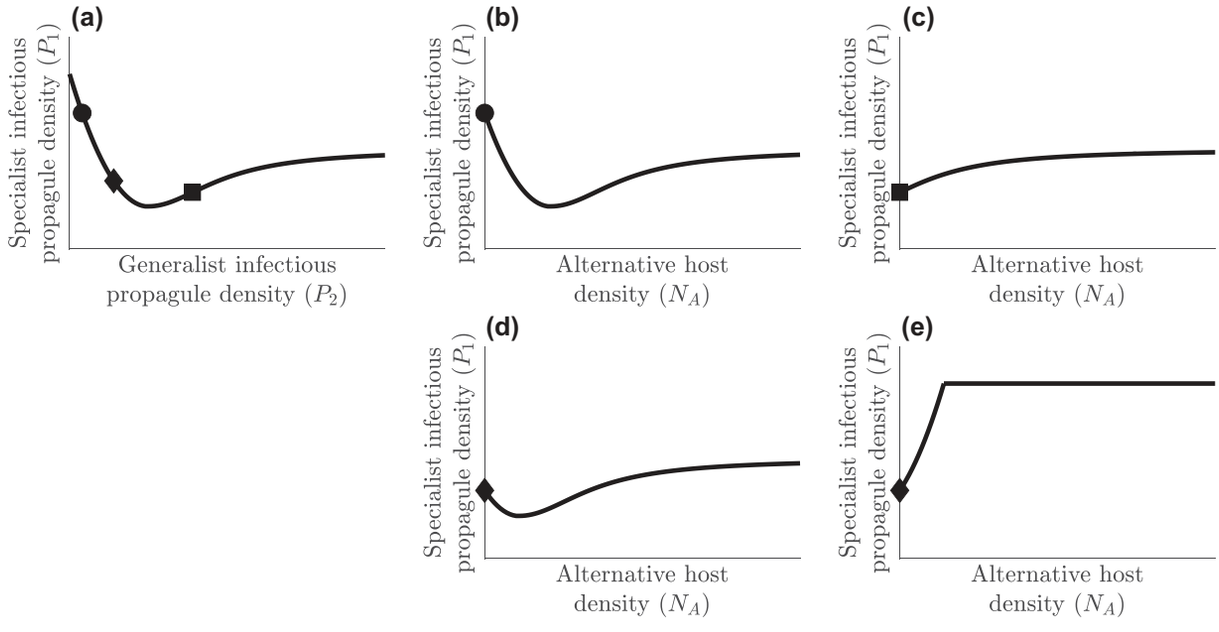

Figure 6: Relationships between alternative host density (N_A) and specialist infectious propagule density (P_1) may be predicted by relationships between generalist (P_2) and specialist (P_1) propagule densities. *a*, Relationship between generalist and specialist propagule densities. Symbols denote generalist infectious propagule density in the absence of the alternative host for the other panels. *b*–*d*, Relationships between N_A and P_1 when the alternative host is a source for the generalist pathogen and the generalist is more (*b*), less (*c*), or equally (*d*) specialized on the alternative host. *e*, Relationships between N_A and P_1 when the alternative host is a sink for the generalist pathogen.

within-host priority effects and whether the alternative host is a source (fig. 6*b*–6*d*) or sink (fig. 6*e*).

The shape of the relationship between alternative host density and specialist infectious propagule density also depends on the degree of specialization of the generalist pathogen. If the generalist pathogen is more specialized on the alternative host, then we expect generalist infectious propagule density to be lower in the absence of alternative host (fig. 6*b*). In this case, the relationship between specialist infectious propagule density and alternative host density will look qualitatively similar to the full relationship between alternative and specialist infectious propagule densities. If the generalist pathogen is more specialized on the focal host, then we expect generalist infectious propagule density to be high in the absence of the alternative host (fig. 6*c*). In this case, the relationship between specialist infectious propagule density and alternative host density will resemble only a small part of the relationship between alternative and specialist infectious propagule densities. If the generalist pathogen is not more specialized on either host, then we expect generalist infectious propagule density to be intermediate in the absence of alternative host (fig. 6*d*, 6*e*). In this case, the relationship between specialist infectious propagule density and alternative host density will (i) resemble one part of the relationship between alternative and specialist infectious propagule densities when the alternative host is a source for the generalist pathogen (fig. 6*d*) and (ii) resemble the complementary part of the relationship between alternative and specialist infectious propagule densities, but with the opposite orientation, when the alternative host is a sink for the generalist pathogen (fig. 6*e*). Altogether, a focal host's risk of infection by a specialist pathogen can strongly depend on the presence of other host species that can be infected by other shared pathogens, and those effects depend on within-host priority effects, the degree of specialization of the generalist pathogen, and whether the alternative host is a source or sink for the generalist pathogen.

The above has implications for understanding the relationships between host species richness and disease. Host species richness–disease relationships are likely to be context dependent (LoGiudice et al. 2008; Randolph and Dobson 2012; Wood et al. 2016; Rohr et al. 2019), and theoretical studies show that the relationships depend on the strength of interspecific host interactions, the competence of each host species, and the pathogen transmission mode (Rudolf and Antonovics 2005; Roberts and Heesterbeek 2018; Cortez 2021; Cortez and Duffy 2021). Our results suggest that predictions about the shapes of host species richness–disease relationships could depend on and be altered by the presence and abundance of other pathogen species in the community. Specifically, in our model the alternative host is a noncompetent species for the specialist pathogen, meaning that the alternative host cannot spread the specialist pathogen. Empirical and theoretical studies (Keesing et al. 2006; Johnson et al. 2008; Hall et al. 2009; O'Regan et al. 2015; Strauss et al. 2015; Dallas et al. 2016) have shown that noncompetent species can reduce disease in a focal host because of reduced transmission. However, if the focal host species and the noncompetent species share a generalist pathogen, then the presence or increased abundance of the noncompetent species can increase or decrease disease in the focal host. Thus, the presence of other pathogens in a community can alter predictions about how gains or losses of noncompetent species affect levels of a focal disease in a focal host.

As a specific example, the host species *Daphnia dentifera* can be infected by the bacterial pathogen *Pasteuria ramosa* and the fungal pathogen *Metschnikowia bicuspidate*. Because of strain specificity, the bacterial pathogen is akin to the specialist pathogen in our model, and the fungal pathogen is akin to the generalist pathogen (Duffy et al. 2010). Empirical estimates of shedding and mortality rates in Clay et al. (2019*b*) show that (i) coinfected individuals have lower shedding rates of the specialist than singly infected individuals and the specialist has a second-arriver advantage in shedding ($\chi_F^1 > \chi_F^{21} > \chi_F^{12}$), (ii) coinfected individuals have roughly equal mortality rates that are much larger than individuals singly infected with the specialist ($m_F^1 < m_F^{21} = m_F^{12}$), and (iii) the shedding rates and mortality rates of individuals infected with the generalist pathogen are roughly equal ($\psi_F^2 = \psi_F^{12} = \psi_F^{21}$, $m_F^2 = m_F^{12} = m_F^{21}$). These parameter conditions qualitatively align with the curve in figure 6*a*. Consequently, if an alternative host of the generalist is present and the alternative host is a source for the generalist pathogen (e.g., like *D. lumholtzi*; Searle et al. 2016), then increased density of the alternative host initially decreases the focal host's risk of infection but eventually causes an increase (fig. 6*d*). Thus, we would predict fewer specialist infections in *D. dentifera* when *D. lumholtzi* density is low and more specialist infection when *D. lumholtzi* density is higher. In contrast, if an alternative host of the generalist is present and the alternative host is a sink for the generalist pathogen (e.g., like *Ceriodaphnia dubia*; Strauss et al. 2015), then increased density of the alternative host always increases the focal host's risk of infection by the specialist (fig. 6*e*). Thus, we would predict more specialist infections in *D. dentifera* whenever *D. lumholtzi* is present. This shows that even though the two alternative host species cannot be infected by the specialist, their different interactions with the generalist pathogen result in different effects on the focal host's risk of being infected by the specialist.

While our results suggest how the presence of other pathogens and their alternative host species can shape

disease risk in a focal host, some caution is advised when applying our results because of the limitations of the model and our approach. One key assumption of the model is that the specialist pathogen can infect only one host species. However, most host-pathogen communities are made of many host species and many pathogen species where the pathogens have overlapping host ranges and most host species can be coinfected by multiple pathogens (Cleaveland et al. 2001; Pedersen et al. 2005; Rigaud et al. 2010). A second key assumption is that the host population sizes are fixed. This implicitly assumes that there are no interspecific interactions between the host species, which removes some of the indirect interactions between pathogens at the between-host level. This assumption may be true in some empirical systems; however, many host species with shared pathogens can interspecifically interact, and theory for multihost systems predicts that those interactions can have large effects on levels of disease (Rudolf and Antonovics 2005; O'Regan et al. 2015; Cortez 2021; Cortez and Duffy 2021). Overall, while additional work is needed to more fully understand the drivers of multihost-multipathogen dynamics, our study provides some insight into how indirect interactions between pathogens shape those dynamics.

Acknowledgments

This work was supported by the National Science Foundation under award DEB-2015280.

Statement of Authorship

Both authors designed the study. J.J. ran the numerical analyzes. M.H.C. did the analytical calculations. J.J. wrote the first draft, and both authors contributed to editing.

Data and Code Availability

The R code for all figures is available on Zenodo (https://doi.org/10.5281/zenodo.6654508; Jiao and Cortez 2022).

References

Abdullah, A. S., C. S. Moffat, F. J. Lopez-Ruiz, M. R. Gibberd, J. Hamblin, and A. Zerihun. 2017. Host–multi-pathogen warfare: pathogen interactions in co-infected plants. Frontiers in Plant Science 8:1806.

Auld, S. K., S. R. Hall, and M. A. Duffy. 2012. Epidemiology of a *Daphnia*-multiparasite system and its implications for the Red Queen. PLoS ONE 7:e39564.

Auld, S. K., S. R. Hall, J. Housley Ochs, M. Sebastian, and M. A. Duffy. 2014. Predators and patterns of within-host growth can mediate both among-host competition and evolution of transmission potential of parasites. American Naturalist 184:S77–S90.

Balmer, O., and M. Tanner. 2011. Prevalence and implications of multiple-strain infections. Lancet Infectious Diseases 11:868–878.

Barker, S. E., I. R. Bricknell, J. Covello, S. Purcell, M. D. Fast, W. Wolters, and D. A. Bouchard. 2019. Sea lice, *Lepeophtheirus salmonis* (Krøyer 1837), infected Atlantic salmon (*Salmo salar* L.) are more susceptible to infectious salmon anemia virus. PLoS ONE 14:e0209178.

Bartholomew, J. L., and P. W. Reno. 2002. The history and dissemination of whirling disease. Pages 3–24 *in* American Fisheries Society symposium. American Fisheries Society, Bethesda, MD.

Ben-Ami, F., L. Mouton, and D. Ebert. 2008. The effects of multiple infections on the expression and evolution of virulence in a *Daphnia*-endoparasite system. Evolution 62:1700–1711.

Bender, E. A., T. J. Case, and M. E. Gilpin. 1984. Perturbation experiments in community ecology: theory and practice. Ecology 65:1–13.

Booth, M. 2006. The role of residential location in apparent helminth and malaria associations. Trends in Parasitology 22:359–362.

Bordes, F., and S. Morand. 2011. The impact of multiple infections on wild animal hosts: a review. Infection Ecology and Epidemiology 1:7346.

Chilvers, G., and E. Brittain. 1972. Plant competition mediated by host-specific parasites—a simple model. Australian Journal of Biological Sciences 25:749–756.

Clay, P. A., M. H. Cortez, M. A. Duffy, and V. H. Rudolf. 2019*a*. Priority effects within coinfected hosts can drive unexpected population-scale patterns of parasite prevalence. Oikos 128:571–583.

Clay, P. A., K. Dhir, V. H. Rudolf, and M. A. Duffy. 2019*b*. Within-host priority effects systematically alter pathogen coexistence. American Naturalist 193:187–199.

Clay, P. A., M. A. Duffy, and V. H. Rudolf. 2020. Within-host priority effects and epidemic timing determine outbreak severity in co-infected populations. Proceedings of the Royal Society B 287: 20200046.

Cleaveland, S., M. K. Laurenson, and L. H. Taylor. 2001. Diseases of humans and their domestic mammals: pathogen characteristics, host range and the risk of emergence. Philosophical Transactions of the Royal Society of London B 356:991–999.

Cortez, M. H. 2021. Using sensitivity analysis to identify factors promoting higher versus lower infection prevalence in multihost communities. Journal of Theoretical Biology 526:110766.

Cortez, M. H., and M. A. Duffy. 2020. Comparing the indirect effects between exploiters in predator-prey and host-pathogen systems. American Naturalist 196:E144–E159.

———. 2021. The context-dependent effects of host competence, competition, and pathogen transmission mode on disease prevalence. American Naturalist 198:179–194.

Dallas, T., R. J. Hall, and J. M. Drake. 2016. Competition-mediated feedbacks in experimental multispecies epizootics. Ecology 97:661–670.

De Roode, J. C., M. E. Helinski, M. A. Anwar, and A. F. Read. 2005. Dynamics of multiple infection and within-host competition in genetically diverse malaria infections. American Naturalist 166:531–542.

de Roos, A. M., and L. Persson. 2013. Population and community ecology of ontogenetic development. Princeton University Press, Princeton, NJ.

de Roos, A. M., T. Schellekens, T. van Kooten, K. van de Wolfshaar, D. Claessen, and L. Persson. 2007. Food-dependent growth leads

to overcompensation in stage-specific biomass when mortality increases: the influence of maturation versus reproduction regulation. American Naturalist 170:E59–E76.

Duffy, M. A., C. E. Cáceres, S. R. Hall, A. J. Tessier, and A. R. Ives. 2010. Temporal, spatial, and between-host comparisons of patterns of parasitism in lake zooplankton. Ecology 91:3322–3331.

Ebert, D. 2005. Ecology, epidemiology, and evolution of parasitism in *Daphnia*. National Library of Medicine, Bethesda, MD.

Ebert, D., M. Lipsitch, and K. L. Mangin. 2000. The effect of parasites on host population density and extinction: experimental epidemiology with *Daphnia* and six microparasites. American Naturalist 156:459–477.

Ezenwa, V. O. 2021. Co-infection and nutrition: integrating ecological and epidemiological perspectives. Pages 411–428 *in* Nutrition and infectious diseases. Springer, Cham.

Ezenwa, V. O., R. S. Etienne, G. Luikart, A. Beja-Pereira, and A. E. Jolles. 2010. Hidden consequences of living in a wormy world: nematode-induced immune suppression facilitates tuberculosis invasion in African buffalo. American Naturalist 176:613–624.

Ezenwa, V. O., and A. E. Jolles. 2011. From host immunity to pathogen invasion: the effects of helminth coinfection on the dynamics of microparasites. Integrative and Comparative Biology 51:540–551.

Fiorello, C. V., M. H. Straub, L. M. Schwartz, J. Liu, A. Campbell, A. K. Kownacki, and J. E. Foley. 2017. Multiple-host pathogens in domestic hunting dogs in Nicaragua's Bosawás Biosphere Reserve. Acta Tropica 167:183–190.

Gao, D., T. C. Porco, and S. Ruan. 2016. Coinfection dynamics of two diseases in a single host population. Journal of Mathematical Analysis and Applications 442:171–188.

Goodman, R. M., and A. F. Ross. 1974. Enhancement by potato virus Y of potato virus X synthesis in doubly infected tobacco depends on the timing of invasion by the viruses. Virology 58:263–271.

Graham, A. L. 2008. Ecological rules governing helminth–microparasite coinfection. Proceedings of the National Academy of Sciences 105:566–570.

Greischar, M. A., H. K. Alexander, F. Bashey, A. I. Bento, A. Bhattacharya, M. Bushman, L. M. Childs, D. R. Daversa, T. Day, C. L. Faust, and M. E. Gallagher. 2020. Evolutionary consequences of feedbacks between within-host competition and disease control. Evolution, Medicine, and Public Health 2020:30–34.

Hall, S. R., C. R. Becker, J. L. Simonis, M. A. Duffy, A. J. Tessier, and C. E. Cáceres. 2009. Friendly competition: evidence for a dilution effect among competitors in a planktonic host–parasite system. Ecology 90:791–801.

Halliday, F. W., R. M. Penczykowski, B. Barrès, J. L. Eck, E. Numminen, and A.-L. Laine. 2020. Facilitative priority effects drive parasite assembly under coinfection. Nature Ecology and Evolution 4:1510–1521.

Halliday, F. W., J. Umbanhowar, and C. E. Mitchell. 2018. A host immune hormone modifies parasite species interactions and epidemics: insights from a field manipulation. Proceedings of the Royal Society B 285:20182075.

Hedrick, R. P., M. A. Adkison, M. El-Matbouli, and E. MacConnell. 1998. Whirling disease: re-emergence among wild trout. Immunological reviews 166:365–376.

Hersh, M. H., R. Vilgalys, and J. S. Clark. 2012. Evaluating the impacts of multiple generalist fungal pathogens on temperate tree seedling survival. Ecology 93:511–520.

Holt, R. D., and A. P. Dobson. 2006. Extending the principles of community ecology to address the epidemiology. Disease Ecology: Community Structure and Pathogen Dynamics 1:6.

Hoverman, J. T., B. J. Hoye, and P. T. Johnson. 2013. Does timing matter? how priority effects influence the outcome of parasite interactions within hosts. Oecologia 173:1471–1480.

Jiao, J., and M. H. Cortez. 2022. Code from: Exploring how a generalist pathogen and within-host priority effects alter the risk of being infected by a specialist pathogen. American Naturalist, Zenodo, https://doi.org/10.5281/zenodo.6654508.

Jiao, J., S. S. Pilyugin, and C. W. Osenberg. 2016. Random movement of predators can eliminate trophic cascades in marine protected areas. Ecosphere 7:e01421.

Johnson, P. T., R. B. Hartson, D. J. Larson, and D. R. Sutherland. 2008. Diversity and disease: community structure drives parasite transmission and host fitness. Ecology Letters 11:1017–1026.

Johnson, P. T. J., D. L. Preston, J. T. Hoverman, J. S. Henderson, S. H. Paull, K. L. D. Richgels, and M. D. Redmond. 2012. Species diversity reduces parasite infection through cross-generational effects on host abundance. Ecology 93:56–64.

Karvonen, A., J. Jokela, and A.-L. Laine. 2019. Importance of sequence and timing in parasite coinfections. Trends in Parasitology 35:109–118.

Keesing, F., R. D. Holt, and R. S. Ostfeld. 2006. Effects of species diversity on disease risk. Ecology Letters 9:485–498.

Lazzaro, B. P., and T. J. Little. 2009. Immunity in a variable world. Philosophical Transactions of the Royal Society B 364:15–26.

LoGiudice, K., S. T. Duerr, M. J. Newhouse, K. A. Schmidt, M. E. Killilea, and R. S. Ostfeld. 2008. Impact of host community composition on Lyme disease risk. Ecology 89:2841–2849.

Lohr, J. N., M. Yin, and J. Wolinska. 2010. Prior residency does not always pay off—co-infections in *Daphnia*. Parasitology 137: 1493–1500.

Mabbott, N. A. 2018. The influence of parasite infections on host immunity to co-infection with other pathogens. Frontiers in Immunology 9:2579.

Meeus, I., M. Pisman, G. Smagghe, and N. Piot. 2018. Interaction effects of different drivers of wild bee decline and their influence on host–pathogen dynamics. Current Opinion in Insect Science 26:136–141.

Mordecai, E. A., K. Gross, and C. E. Mitchell. 2016. Within-host niche differences and fitness trade-offs promote coexistence of plant viruses. American Naturalist 187:E13–E26.

Nørgaard, L. S., B. L. Phillips, and M. D. Hall. 2019. Infection in patchy populations: contrasting pathogen invasion success and dispersal at varying times since host colonization. Evolution Letters 3:555–566.

O'Regan, S. M., J. E. Vinson, and A. W. Park. 2015. Interspecific contact and competition may affect the strength and direction of disease-diversity relationships for directly transmitted microparasites. American Naturalist 186:480–494.

Pedersen, A. B., S. Altizer, M. Poss, A. A. Cunningham, and C. L. Nunn. 2005. Patterns of host specificity and transmission among parasites of wild primates. International Journal of Parasitology 35:647–657.

Petney, T. N., and R. H. Andrews. 1998. Multiparasite communities in animals and humans: frequency, structure and pathogenic significance. International Journal for Parasitology 28:377–393.

Pulkkinen, K., L.-R. Suomalainen, A. Read, D. Ebert, P. Rintamäki, and E. Valtonen. 2010. Intensive fish farming and the evolution of pathogen virulence: the case of columnaris disease in Finland. Proceedings of the Royal Society B 277:593–600.

Randolph, S. E., and A. D. M. Dobson. 2012. Pangloss revisited: a critique of the dilution effect and the biodiversity-buffers-disease paradigm. Parasitology 139:847–863.

Rigaud, T., M. Perrot-Minnot, and R. J. F. Brown. 2010. Parasite and host assemblages: embracing the reality will improve our knowledge of parasite transmission and virulence. Proceeding of the Royal Society B 277:3693–3702.

Roberts, M., and J. Heesterbeek. 2018. Quantifying the dilution effect for models in ecological epidemiology. Journal of the Royal Society Interface 15:20170791.

Rohr, J. R., D. J. Civitello, F. W. Halliday, P. J. Hudson, K. D. Lafferty, C. L. Wood, and E. A. Mordecai. 2019. Towards common ground in the biodiversity–disease debate. Nature Ecology and Evolution 4:24–33.

Romansic, J. M., P. T. Johnson, C. L. Searle, J. E. Johnson, T. S. Tunstall, B. A. Han, J. R. Rohr, and A. R. Blaustein. 2011. Individual and combined effects of multiple pathogens on pacific treefrogs. Oecologia 166:1029–1041.

Rudolf, V. H. W., and J. Antonovics. 2005. Species coexistence and pathogens with frequency-dependent transmission. American Naturalist 166:112–118.

Sandoval-Aguilar, J. A., A. W. Guzmán-Franco, J. K. Pell, S. J. Clark, R. Alatorre-Rosas, M. T. Santillán-Galicia, and G. Valdovinos-Ponce. 2015. Dynamics of competition and co-infection between *Zoophthora radicans* and *Pandora blunckii* in *Plutella xylostella* larvae. Fungal Ecology 17:1–9.

Seabloom, E. W., E. T. Borer, K. Gross, A. E. Kendig, C. Lacroix, C. E. Mitchell, E. A. Mordecai, and A. G. Power. 2015. The community ecology of pathogens: coinfection, coexistence and community composition. Ecology Letters 18:401–415.

Searle, C. L., M. H. Cortez, K. K. Hunsberger, D. C. Grippi, I. A. Oleksy, C. L. Shaw, S. B. de la Serna, C. L. Lash, K. L. Dhir, and M. A. Duffy. 2016. Population density, not host competence, drives patterns of disease in an invaded community. American Naturalist 188:554–566.

Sorenson, D. K., and M. H. Cortez. 2021. How intra-stage and inter-stage competition affect overcompensation in density and hydra effects in single-species, stage-structured models. Theoretical Ecology 14:23–39.

Strauss, A. T., D. J. Civitello, C. E. Cáceres, and S. R. Hall. 2015. Success, failure and ambiguity of the dilution effect among competitors. Ecology Letters 18:916–926.

Wolinska, J., and K. C. King. 2009. Environment can alter selection in host–parasite interactions. Trends in Parasitology 25:236–244.

Wood, C. L., K. D. Lafferty, G. DeLeo, H. S. Young, P. J. Hudson, and A. M. Kuris. 2016. Does biodiversity protect humans against infectious disease? reply. Ecology 97:536–545.

Yodzis, P. 1988. The indeterminacy of ecological interactions. Ecology 69:508–515.

Associate Editor: Matthew J. Ferrari
Editor: Daniel I. Bolnick

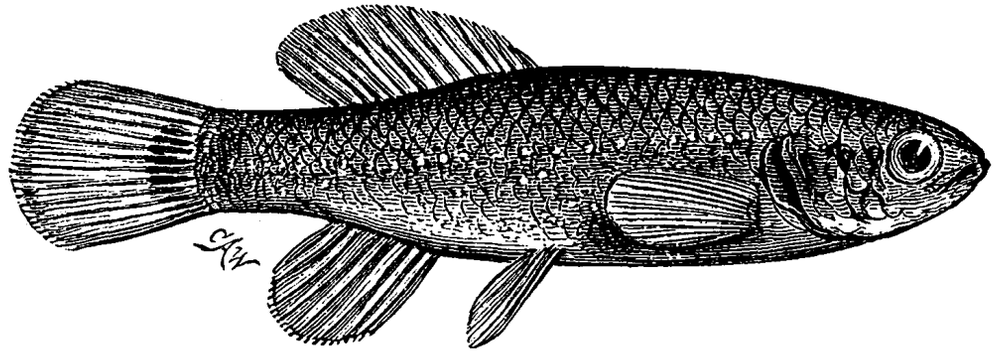

"On the 16th of March we found females of the Mud Minnow (*Melanura limi*), in clear, cold, running water. They were much distended with large masses of orange-colored eggs. . . . On the other hand they are themselves exposed to attacks from a voracious animal, which takes advantage of their lying buried in the mud. We refer to the odoriferous Cinosternoid (*Ozotheca odorata*). This turtle appears to be able to discover the whereabouts of the mud-minnows without alarming them; and cautiously approaching from behind, they seize the head of the fish that is scarcely extruded from the mud." From "Mud-Loving Fishes" by Charles C. Abbott (*The American Naturalist*, 1870, 4:385–391).